Enhanced Diffusion, Chemotaxis, and Pumping by Active Enzymes: Progress toward an Organizing Principle of Molecular Machines

R. Dean Astumian*

Department of Physics, The University of Maine, 5709 Bennett Hall, Orono, Maine 04469-5709, United States

ABSTRACT Active enzymes diffuse more rapidly than inactive enzymes. This phenomenon may be due to catalysis-driven conformational changes that result in "swimming" through the aqueous solution. Recent additional work has demonstrated that active enzymes can undergo chemotaxis toward regions of high substrate concentration, whereas inactive enzymes do not, and, further, that active enzymes immobilized at surfaces can directionally pump liquids. In this Perspective, I will discuss these phenomena in light of Purcell's work on directed motion at low Reynold's number and in the context of microscopic reversibility. The conclusions suggest that a deep understanding of catalytically driven enhanced diffusion of enzymes and related phenomena can lead toward a general organizing principle for the design, characterization, and operation of molecular machines.

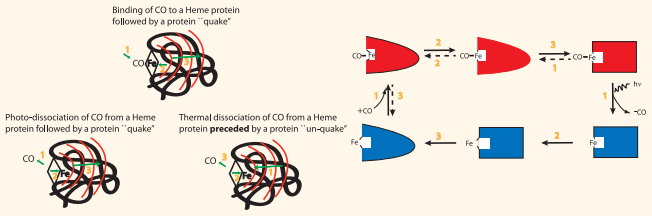

Enzymes often undergo significant conformational changes as they bind substrate and release product[1] while carrying out their catalytic function. In a viscous solvent such as water, each shape change causes a translation through the medium. Purcell, in a seminal paper, "Life at Low Reynolds Number",[2] discussed the constraints on *directed* movement arising from cyclic shape changes of an object for which the inertial force is negligible in comparison to the viscous drag force, the ratio of the two forces being the Reynold's number. In order to make net progress in a particular direction, the shape changes must occur in a nonreciprocal cycle, where the sequence of changes does not retrace itself as the object departs from and then returns to some reference shape. This conclusion has been termed the "scallop theorem", based on Purcell's discussion of the mechanism of motion of a scallop that works at medium and high Reynold's number but fails at low Reynold's number. The mechanism by which self-propulsion occurs at low Reynold's number is geometric rather than dynamical—the distance traveled per cycle of shape changes is independent of how rapidly any of the changes occur.[3]

Muddana *et al.*[4] recently demonstrated experimentally that an active enzyme, urease, diffuses more rapidly than the same enzyme inactivated by the inhibitor pyrocatechol, demonstrating that catalysis leads to enhanced diffusion (see Figure 1a) and suggesting the possibility that this enhanced diffusion arises because of nonreciprocal conformational changes. It must be noted that Lauga[5] has shown that even reciprocal shape changes can give rise to enhanced diffusion, so the observation reported by Muddana *et al.*[4] does not necessarily show that the conformational changes during catalysis by urease must occur in nonreciprocal cycles. Further, Muddana *et al.*[4] also suggested that the mechanism may involve self-electrophoresis since the product of the reaction catalyzed by urease is charged.

In this issue of *ACS Nano*, Dey *et al.*[6] report on the experimental observation of a phenomenon that is closely related to enhanced diffusion, chemotaxis by active enzymes in the presence of a gradient of their substrate, as schematically shown in Figure 1b. A continuous flow of substrate through the upper channel maintains a gradient of substrate. A mixture of active

* Address correspondence to astumian@maine.edu.

Published online December 23, 2014
10.1021/nn507039b

© 2014 American Chemical Society

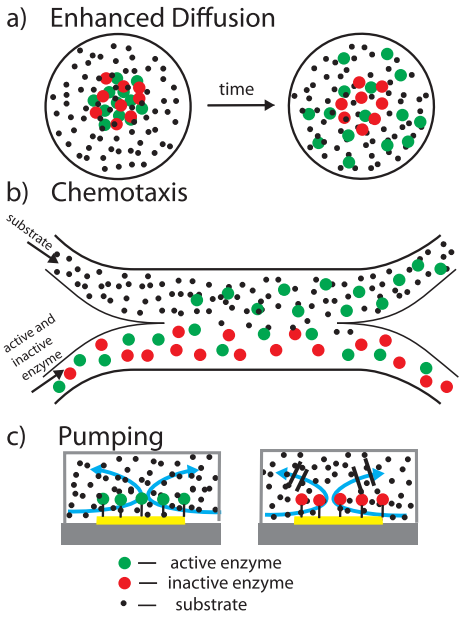

Figure 1. Illustration of three phenomena displayed by active enzymes but not by inactive enzymes: (a) enhanced diffusion, (b) chemotaxis, and (c) pumping.

and inactive enzyme flows through the lower channel. Because the diffusion constant of the active enzyme increases with substrate concentration, the active enzyme preferentially moves toward the region of high substrate concentration and the solution that flows out through the upper channel is significantly enriched with active relative to inactive enzyme. By use of chemotaxis due to enhanced diffusion, it is thus possible to separate enzymes based solely on their chemical activity rather than on their physical properties.

A third related phenomenon, pumping of solvent by DNA polymerase immobilized at a surface, was studied by Sengupta *et al.*[7] The active enzyme in the presence of the important cofactor Mg^{2+}, single-stranded DNA, and free nucleotide bases as substrate was shown to have a significantly larger diffusion constant than either a mutated enzyme incapable of carrying out multiple cycles of catalysis or the wild-type enzyme without Mg^{2+}. The active enzyme was also shown to undergo chemotaxis toward regions of higher Mg^{2+} concentration in an experiment similar to that illustrated in Figure 1b. The polymerase remained able to carry out its catalytic function when immobilized on a gold surface and, in doing so, caused net pumping of liquid as shown schematically in Figure 1c. Pumping was not seen with inactive enzyme nor with enzyme in the absence of the Mg^{2+} cofactor. The pumping was observed to reverse direction relative to the glass surface when the pump setup is inverted such that the gold surface was at the top of the chamber. This reversal is consistent with a mechanism in which pumping results in a decrease in the fluid density near the surface, and the mechanism seems to require a nonreciprocal cycle of conformational states.

> By use of chemotaxis due to enhanced diffusion, it is thus possible to separate enzymes based solely on their chemical activity rather than on their physical properties.

The takeaway message of this Perspective is that almost any enzyme can, in principle, function as a molecular machine, and that consideration of the phenomena of catalysis-enhanced diffusion, chemotaxis, and pumping in the context of the symmetry constraints provided by Purcell's scallop theorem[2] and by Onsager's principle of microscopic reversibility[8] can provide a general understanding of the organizing principles governing the design, operation, and characterization, of **molecular** machines.

In order to understand how catalysis can lead to enhanced diffusion, chemotaxis, and pumping, let us consider one specific physical mechanism for "swimming" at low Reynold's number.

> Almost any enzyme can, in principle, function as a molecular machine.

Swimming at Low Reynold's Number. In a classic paper,[2] Purcell pointed out that many mechanisms of directed motion that we take for granted at the macroscopic scale involve inertia and are hence ineffective when viscous damping is large. For example, an animal that slowly fills a cavity with water and then rapidly squirts the water out will undergo net motion in the direction opposite to that in which the water is squirted out of the cavity. This mechanism takes advantage of the glide induced when the water is rapidly squirted out of the cavity. When viscous drag dominates inertia, however, this mechanism can no longer work since the motion induced when the water is slowly sucked into the cavity is opposite and equal in magnitude to the motion caused when the liquid is squirted out, irrespective of how rapidly the water squirts out—there is no glide. The ratio of the inertial force to the viscous drag force is

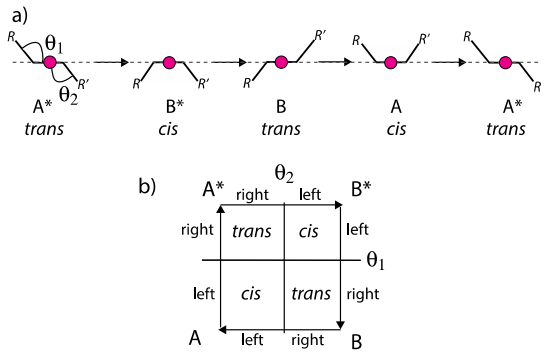

Figure 2. Illustration of Purcell's three-link swimmer. The critical spatial symmetry breaking occurs because those motions of the swimmer that tend to move the swimmer to the left occur when the left and right arms are both on the same side of the middle arm, whereas those motions that tend move the swimmer to the right occur when the left and right arms are on opposite sides of the line containing the middle arm.

known as the Reynold's number. The Reynold's number for bacteria and anything smaller moving in water is very low and necessitates a different mechanism for producing net motion in a particular direction. The classic example of motion at low Reynold's number posited by Purcell is swimming by a three-link swimmer device (Figure 1), where the links move relative to one another by some unspecified mechanism. The basic idea is that the "swimmer" undergoes a cycle of changes in which the motions going from one state to another do not retrace themselves when the device returns to its original state. The origin of the symmetry breaking is clear when we make a parametric plot of the two angles θ_1 and θ_2 against each other, as shown in Figure 2b. Motion of R or R' up or down and to the right moves the center of mass (magenta circle) of the swimmer to the left, and motion of R or R' up or down and to the left moves the center of mass to the right.

We see in Figure 2b that those motions tending to move the center of mass to the right occur when R and R' are on opposite sides of the dashed line containing the central link (*trans*), while those motions that tend to move the center of mass to the left occur when R and R' are on the same side of the of the dashed line (*cis*). This difference in hydrodynamic coupling between the two cases is sufficient to allow net directed motion through a cycle A* → B* → B → A → A*.

Now, let us explore more deeply the constraints of the temporal symmetry known as microscopic reversibility[9] on the mechanism by which a nonreciprocal cycle through conformational states can be achieved.

Nonreciprocal Conformational Cycles and CO Binding to Myoglobin. Consider the binding of carbon monoxide to myoglobin shown in Figure 3.

After CO attachment to the heme group of myoglobin, the iron moves into the plane of the heme, and then a long-range conformational change propagates from the heme group outward. It is natural to hypothesize that after CO dissociation in the reverse debinding process the heme group returns to the out-of-plane configuration, followed by a global conformational change to restore the protein to its original unbound structure. This common sense order of local change followed by global change in the debinding process is supported by experiments of Frauenfelder and colleagues in which CO is photochemically dissociated from myoglobin. Their results led Ansari *et al.*[10] to conclude that "binding or dissociation of a ligand from the heme iron causes a protein quake". This conclusion, however, when applied to thermal (not photochemical) processes, is not consistent with the principle of microscopic reversibility by which the mechanism for a reaction is independent of its direction (http://goldbook.iupac.org/):

> *"In a reversible reaction, the mechanism in one direction is exactly the reverse of the mechanism in the other direction. This does not apply to reactions that begin with a photochemical excitation."*

Counterintuitive though it may be, thermal dissociation must, on average, occur by an "un-quake" preceding the return of the iron to the plane of the heme and only then by release of CO. Unlike photochemical processes, binding and thermal dissociation of any ligand (including ATP) to any macromolecule (including proteins) must occur by the microscopic reverses of one another. The traditional picture of macromolecular dynamics involves "nonequilibrium" functionally important motions[10]—power strokes, protein quakes, *etc.*—that are separate from equilibrium conformational fluctuations. However, the physical motions following ligand binding, catalytic conversion, and dissociation of ligands are all equilibrium processes[11] irrespective of the bulk chemical potentials of the ligands.

The impossibility of achieving a conformational cycle in which the backward path is not, on average, the microscopic reverse of the forward path by thermal binding/dissociation of a single ligand is very important—any molecule that moves between two conformationally distinct states by different pathways in the forward and backward direction is a "low Reynolds number swimmer" as described by Purcell.[2] If such a nonreciprocal cycle could be driven by the binding and release of a single ligand, the Second Law of Thermodynamics would be violated since such a "swimmer" can, when constrained in an appropriate topology, function as a molecular machine. Hence, in designing molecular machines, it is necessary to understand how to achieve a nonreciprocal conformational cycle and, thereby, to understand how the

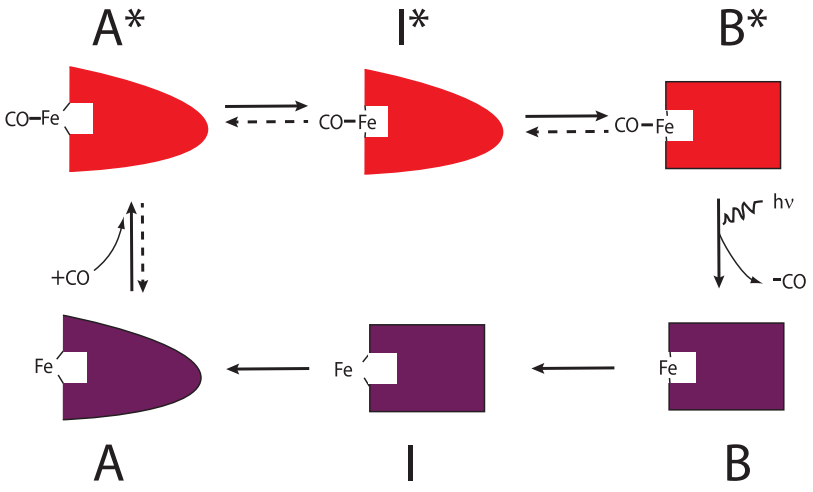

Figure 3. Carbon monoxide binding to myoglobin. After binding CO, the iron moves into the plane of the heme group. This local configuration change is followed by a global conformational change to the stable CO-bound state in the upper right corner (B*). Macroscopic intuition suggests that dissociation should also proceed from local to global, by a so-called protein quake in which dissociation of the CO allows the local change in which iron moves out of the plane of the heme group, followed by a global rearrangement in which the conformation of the protein returns to the minimum energy configuration for the unbound state. This macroscopic intuition is validated by flash photolysis experiments in which this order is observed to occur experimentally. Nevertheless, microscopic reversibility requires that thermal (as opposed to photochemical) dissociation of carbon monoxide must occur preferentially by the microscopic reverse of the binding process, as illustrated by the dashed arrows.

input of energy can be used to circumvent the constraints of microscopic reversibility.

The Constraints of Microscopic Reversibility—Optical *versus* Chemical Driving. Microscopic reversibility constrains the ratio of forward and reverse rate constants for thermally activated transitions (each denoted by "*k*") to be proportional to the exponential of the energy difference between the states

$$\frac{k_{ij}}{k_{ji}} = A_{ij} e^{\Delta U^0_{ij}/k_B T} \qquad (1)$$

where *i* and *j* are any two states. The proportionality constant A_{ij} may involve, for example, the chemical potential of some ligand (such as S or P) that binds in the process or the effect of external fields or deviations of the thermodynamic parameters away from the standard conditions under which ΔU^0 is evaluated. The proportionality constant depends on the specific path by which a molecule in state "*i*" undergoes transition to state "*j*" and *vice versa*. The factor $e^{(\Delta U^0_{ij})/(k_B T)}$, however, is path-independent.

For a photochemical reaction, the ratio of forward to backward transition constants (each denoted by "ω") calculated from the relationship between absorption, spontaneous emission, and stimulated emission by Einstein[12] is

$$\frac{\omega_{ij}}{\omega_{ji}} = \frac{g_i}{g_j} \frac{\rho(\nu_{ij})}{\left[\frac{8\pi h \nu_{ij}^3}{c^3} + \rho(\nu_{ij})\right]} \qquad (2)$$

where *i* and *j* are any two states, $\rho(\nu_{ij})$ is the radiation density at frequency $\nu_{ij} = U_{ij}/h$, where *h* is Planck's constant, and g_i and g_j are the degeneracies of states "*i*" and "*j*", respectively. For bright light at frequency ν_{ij}, we have $g_i^{-1}\omega_{ij} = g_j^{-1}\omega_{ji}$. Note that when we insert the expression for the photon density of a blackbody (bb) radiator at the temperature *T*, $\rho_{bb}(\nu_{ij}) = 8\pi h \nu_{ij}^3 c^{-3}(e^{(\Delta U_{ij})/(k_B T)} - 1)^{-1}$, we find $g_i^{-1}\omega_{ij} = g_j^{-1}\omega_{ji} e^{(\Delta U_{ij})/(k_B T)}$. However, the proportionality to the exponential of the energy difference between states *i* and *j* for a light-driven process holds only for the Planck blackbody distribution function. In contrast, the proportionality to the exponential of the energy difference between states *i* and *j* in eq 1—microscopic reversibility—holds for all thermally activated processes irrespective of whether any chemical driving is or is not at equilibrium or whether there is an external force acting. Only the prefactor A_{ij} depends on the external conditions.

These different constraints for thermal *versus* photochemical transitions suggest different design principles for optically driven *versus* chemically driven cycles. To see how this works out, let us compare a conformational cycle in which the vertical transitions between the nonstar and star states are driven by light (Figure 4a) with a cycle in which the vertical transitions between the nonstar and star states are driven by a catalyzed chemical reaction (Figure 4b).

The systems can be set up such that each completion of the cycle in the clockwise direction A* → B* → B → A → A* does mechanical work, W_{mech}, on the environment[13] (*e.g.*, lifts a weight or stretches a spring), and each completion of the cycle in the counterclockwise direction A* → A → B → B* → A* absorbs and dissipates mechanical work, W_{mech}, from the environment (*e.g.*, a weight is lowered or the spring relaxes). For the chemically driven cycle in Figure 4b, we have borrowed Huxley's notation[14] in which each cycle of f_i and g_j* for *i* and *j* = A or B involves catalysis of some

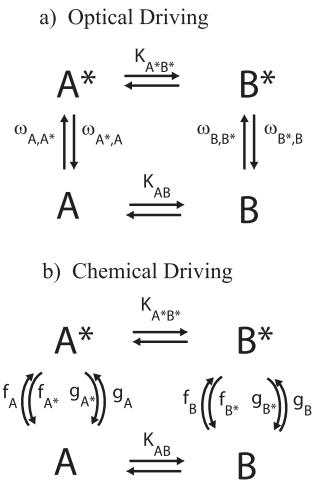

Figure 4. Two mechanisms by which net cycling through several conformational states can be driven. (a) Optical driving in which rates of absorption/emission of light (ω_{ij}) are constrained by the Einstein relations between absorption, spontaneous emission, and stimulated emission of light (eq 2). (b) Chemical driving, where each pair of forward and reverse frequencies obeys microscopic reversibility (eq 1).

substrate S to product P driven by the free energy change $\Delta\mu = \mu_S - \mu_P$. These processes are not the microscopic reverses of one another, but rather f_i^* is the microscopic reverse of f_i and g_j is the microscopic reverse of g_j^*. The constraints of microscopic reversibility on the "*f*" and "*g*" processes can be summarized as

$$\frac{f_A g_{A^*}}{g_A f_{A^*}} = \frac{f_B g_{B^*}}{g_B f_{B^*}} = e^{\Delta\mu/k_BT}$$

$$\frac{f_A f_{B^*}}{f_B f_{A^*}}\frac{K_{A^*B^*}}{K_{AB}} = \frac{g_A g_{B^*}}{g_B g_{A^*}}\frac{K_{A^*B^*}}{K_{AB}} = e^{-W_{mech}/k_BT} \quad (3)$$

The ratio of completions of clockwise to counterclockwise cycles for Figure 4a,b is the product of clockwise rate constants divided by the product of the counterclockwise rate constants. For the optically driven cycle, this ratio is

$$\left(\frac{N_{cw}}{N_{ccw}}\right)_{opt} = \frac{\omega_{A,A^*}\omega_{B^*,B}K_{A^*B^*}}{\omega_{A^*,A}\omega_{B,B^*}K_{AB}} \approx e^{[(\Delta U_{A^*B^*} - \Delta U_{AB}) - W_{mech}]/k_BT} \quad (4)$$

where $\Delta U_{ij} = U_i - U_j$ is the energy difference between states *i* and *j* and where the approximation holds for bright light. The predominant direction of cycling is governed by the relative energies of the states, as well as by W_{mech}. The mechanism is described as an energy ratchet[15] because in the excited (*) state, B* is more stable than A*, whereas in the ground state, A is more stable than B. The same results hold when the system is driven externally where the thermodynamic parameters are caused to fluctuate alternately, favoring the star and nonstar states.[16]

For the chemically driven cycle, the ratio of clockwise to counterclockwise cycles is

$$\left(\frac{N_{cw}}{N_{ccw}}\right)_{chem} = \frac{(f_A + g_A)(f_{B^*} + g_{B^*})K_{A^*B^*}}{(f_{A^*} + g_{A^*})(f_B + g_B)K_{AB}} \approx e^{[(\Delta E_B^\dagger - \Delta E_A^\dagger) - W_{mech}]/k_BT} \quad (5)$$

where $\Delta E_i^\dagger = E_{i,f}^\dagger - E_{i,g}^\dagger$ is the difference in the activation barriers for the *f* and *g* processes at site *i* = A,B, and $e^{(\Delta E_B^\dagger - \Delta E_A^\dagger)/(k_BT)} = (f_A g_B)/(f_B g_A)$. The approximation holds for the case of very strong chemical driving, that is, in the limit that $\Delta\mu \to \infty$, and is derived using the constraints of microscopic reversibility given in eq 3. The ratio of clockwise to counterclockwise cycles is independent of the energies of the states and depends only on the transition state energies. Note that if some of the "*f*" and "*g*" rates are simply assigned to be zero in eq 5, one can easily arrive at the opposite, wrong, conclusion that the ratio of clockwise to counterclockwise cycle completions does depend on ΔU_{AB} and $\Delta U_{A^*B^*}$. It is never thermodynamically correct simply to set a rate to be zero, and doing so can lead to qualitatively incorrect conclusions even if the quantitative magnitude of the error introduced into numerical calculations of kinetic behavior under particular experimental conditions is vanishingly small.

This mechanism describes an information ratchet[17] in which the catalysis is kinetically gated by allosteric interactions such that process "*f*" is fast and "*g*" is slow between states A and A*, and process "*g*" is fast and process "*f*" is slow between states B and B*, both at and away from thermodynamic equilibrium. At equilibrium, however, it is equally likely for the reaction to proceed either in the direction where S is converted to P concomitant with completion of a clockwise cycle or in the direction where P is converted to S concomitant with completion of a counterclockwise cycle. Directional cycling requires input of energy. Net clockwise cycling in the case described above occurs only if $\Delta\mu > 0$.

Two-Dimensional Potential Energy Surface of the F_1-ATP Synthase. We can appreciate the generality of the independence of the directionality of motion on the state energies in terms of a recent computational model of a two-dimensional potential energy surface for the F_1-ATP synthase[18] shown in Figure 5a and the corresponding expanded kinetic lattice model[19] shown in Figure 5b. The low-energy path running from the lower left to the upper right corner shows how ATP hydrolysis that drives the motion from left to right couples to drive clockwise rotation from bottom to top. In Figure 5a, it is clear that the sense of rotation driven by ATP hydrolysis does not change if the energies of states A/C and B are exchanged, whereas if the energies of the transition states $\mathscr{E}_L$ and $\mathscr{E}_R$ are exchanged, the sense of rotation changes from clockwise to counterclockwise. A kinetic lattice model for the process is shown in Figure 5b, where the transitions between the states are color-coded to the energies of the saddle points (transition states) in Figure 5a. Two periods are shown in each direction in Figure 5b, whereas only one period is shown in Figure 5a and is indicated in Figure 5b by the dashed box.

Irrespective of how many states are involved in the kinetic lattice describing a molecular machine, there is, by symmetry, a one-to-one correspondence between forward ($\mathscr{F}$)

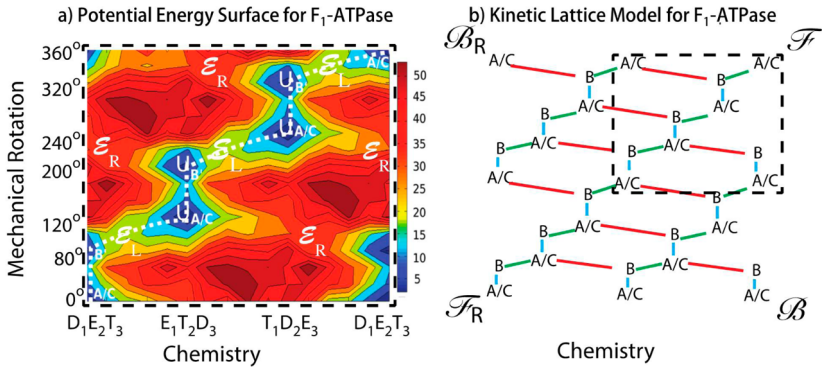

Figure 5. (a) Potential energy surface for ATP-driven rotation of the F_1-ATPase derived from calculation based on the crystal structure of Walker. Energies are given in kcal/mol. The energy surface is redrawn with permission from ref 18. Copyright 2011 National Academy of Sciences. (b) Corresponding kinetic lattice model for the process, where the section enclosed in the dashed box corresponds to that part of the periodic energy surface shown in (a).

paths in which substrate is converted to product (ATP is hydrolyzed for the case of F_1-ATPase) and the machine makes a forward mechanical step (rotates clockwise), backward ($\mathscr{B}$) paths in which substrate is converted to product and the machine makes a backward mechanical step, forward reverse ($\mathscr{F}_R$) paths in which product is converted to substrate (ATP is synthesized) and the machine makes a backward mechanical step, and backward reverse ($\mathscr{B}_R$) paths in which product is converted to substrate and the machine makes a forward mechanical step. The ratios between probabilities for paths that are the microscopic reverses of one another, $P(\mathscr{F})/P(\mathscr{F}_R)$ and $P(\mathscr{B})/P(\mathscr{B}_R)$, are thermodynamic identities. On the other hand, the ratio $P(\mathscr{B})/P(\mathscr{F})$ depends on the structure of the molecular machine through the transition state energies. The selection between paths $\mathscr{F}$ and $\mathscr{B}$ is the sole determinant of the intrinsic (zero load) directionality of the machine. There are also slip paths in which the motor takes a step without conversion between substrate and product and futile cycle paths in which the motor catalyzes conversion between substrate and product without stepping. These slip and futile cycle paths can only reduce the intrinsic stepping ratio, efficiency, stopping force, and stoichiometry (number of steps per fuel molecule) of the motor and do not impact the preferred direction of stepping.

For the F_1-ATPase, the ratio $P(\mathscr{B})/P(\mathscr{F}) = \exp(-\Delta\mathscr{E}/k_BT)$, where $\Delta\mathscr{E} = 2(\mathscr{E}_R - \mathscr{E}_L)$. Since $\Delta\mathscr{E} \approx 40$ kcal/mol is significantly greater than $\Delta\mu \approx 12$ kcal provided by ATP hydrolysis, a large torque that drives counterclockwise rotation of the F_1-ATPase drives synthesis of ATP by the pathway $\mathscr{F}_R$ and adding ATP will inhibit counterclockwise rotation. In contrast, the difference in barrier energies for the $\mathscr{F}$ and $\mathscr{B}$ paths for kinesin seems to be less than 10 kcal/mol, and thus in the presence of an external force that is sufficiently strong to cause backward stepping, the pathway $\mathscr{B}$ is favored over the pathway $\mathscr{F}_R$ and added ATP will stimulate back-stepping as predicted[19] and experimentally observed[21] for kinesin.

The result that the directionality of mechanical motion induced by chemical catalysis is independent of the state energies and governed entirely by transition state energies is general.[20] The principle of microscopic reversibility guarantees that the dynamics of a molecular machine in which directed mechanical movement is coupled to a catalyzed chemical reaction such as ATP hydrolysis can be described in terms of motion on a single potential energy landscape—a scalar field. On such an energy surface, the sign of the coupling—the directionality of motion induced along one coordinate by a "generalized force" acting along an orthogonal coordinate—depends only on the saddle point energies and not on the energies of the minima or maxima. This conclusion arises from the fact that the energy increases in every direction away from a minimum, while at the saddle points, there is one direction along which the energy decreases and perpendicular, [orthogonal] to that direction the energy increases. Thus, there is an inherent selection of a preferred path at each saddle point. The overall preferred pathway for motion is determined by the relative energies of the different saddle points. The direction of motion on this overall preferred path when the external force or torque is zero is determined solely by mass action—that is, by the sign of the $\Delta\mu$ for the chemical reaction.

It is tempting, but wrong, to attempt to describe the effect of $\Delta\mu$ in analogy with the effect of force acting along the chemical coordinate of the reduced potential. The effect of binding and release of any ligand (substrate or product) is local, and concentrations of substrate and product impact only the probability to bind substrate *versus* product when the active site is unoccupied and do not influence the energetics at the single-molecule level. The effect of $\Delta\mu$ is known as mass action.

There is a better case to be made for modeling the effect of an externally applied force or torque as a tilt

along the mechanical coordinate, but even then, we must realize that the external force or torque influences the relative energies of all points on the reduced potential to varying degrees. The effect of the force or torque cannot generally be described as additive except between periodically related points.

CONCLUSIONS AND PROSPECTS

The literature on molecular machines is replete with analogies between molecular motors and macroscopic machines, where the former are described as wind-up toys,[22] their motions are likened to judo throws,[23] and the effect of ATP hydrolysis is described as being equivalent to violent kicks.[24] Further, animated movies of biomolecular motors often represent ATP hydrolysis as a flash of light. These depictions are consistent with what Bustamante has termed the "mechanical paradigm" for molecular machines,[25] echoing the classic holy grail of attaining understanding of molecular machines in terms of Newton's equations of motion.

A strongly contrasting picture, loosely describable as a Brownian motor paradigm,[26,27] has emerged where the constructive role of thermal noise is emphasized and the mechanism can be described as a random walk on a lattice of states.[19] Instead of using energy to cause forward movement, the motion of a Brownian motor is caused by thermal noise, which *a priori* occurs randomly in all directions. The input chemical energy is used to prevent backward motion by opening and closing gates depending on the chemical state of the machine rather than to cause forward motion.

As pointed out by Mukherjee and Warshel,[18] the potential energy surface for any molecular machine completely determines its functionality and coupling. Recent work on catalysis-induced chemotaxis, enhanced diffusion, and pumping by single enzymes shows that almost all enzymes can, in principle, function as molecular motors, and that the fundamental mechanisms point to a geometric picture where the enzyme is shepherded through a cycle of states rather than to the mechanical picture in which the machine is pushed through its cycle of states by power strokes. Using this Perspective, we can go beyond Warshel and Mukherjee's simple recognition of the importance of the energy landscape to the understanding that the specific features of the energy landscape that govern the coupling are the saddle points—the transition states—as predicted by a Brownian motor model and not the energy differences between the states as predicted by the mechanical paradigm in which the "power stroke" plays a crucial role. Consideration of the phenomena of enhanced diffusion and chemotaxis by enzymes, as well as active pumping when enzymes are immobilized on a surface, illuminates the importance of microscopic reversibility as an organizing principle of molecular machines by which the motion of any chemically driven molecular machine can be described in terms of diffusion on a potential energy landscape.

Conflict of Interest: The authors declare no competing financial interest.

Acknowledgment. The author is grateful for very useful discussions with Prof. Ayusman Sen (Penn State) and to Prof. Arieh Warshel for permission to use Figure 5a.

REFERENCES AND NOTES

1. Nashine, V. C.; Hammes-Schiffer, S.; Benkovic, S. J. Coupled Motions in Enzyme Catalysis. *Curr. Opin. Chem. Biol.* **2010**, *14*, 644–651.
2. Purcell, E. M. Life at Low Reynolds Number. *Am. J. Phys.* **1977**, 1–9.
3. Shapere, A.; Wilczek, F. Self-Propulsion at Low Reynolds Number. *Phys. Rev. Lett.* **1987**, *58*, 2051–2054.
4. Muddana, H. S.; Sengupta, S.; Mallouk, T. E.; Sen, A.; Butler, P. J. Substrate Catalysis Enhances Single-Enzyme Diffusion. *J. Am. Chem. Soc.* **2010**, *132*, 2110–2111.
5. Lauga, E. Enhanced Diffusion by Reciprocal Swimming. *Phys. Rev. Lett.* **2011**, *106*, 178101.
6. Dey, K. K.; Das, S.; Poyton, M. F.; Sengupta, S.; Butler, P. J.; Cremer, P. S.; Sen, A. Chemotactic Separation of Enzymes. *ACS Nano* **2014**, 10.1021/nn504418u.
7. Sengupta, S.; Spiering, M. M.; Dey, K. K.; Duan, W.; Patra, D.; Butler, P. J.; Astumian, R. D.; Benkovic, S. J.; Sen, A. DNA Polymerase as a Molecular Motor and Pump. *ACS Nano* **2014**, *8*, 2410–2418.
8. Onsager, L.; Machlup, S. Fluctuations and Irreversible Processes. *Phys. Rev.* **1953**, *91*, 1505–1512.
9. Astumian, R. D. Microscopic Reversibility as the Organizing Principle of Molecular Machines. *Nat. Nanotechnol.* **2012**, *7*, 684–688.
10. Ansari, A.; Berendzen, J.; Bowne, S. F.; Frauenfelder, H.; Iben, I. E.; Sauke, T. B.; Shyamsunder, E.; Young, R. D. Protein States and Proteinquakes. *Proc. Natl. Acad. Sci. U.S.A.* **1985**, *82*, 5000–5004.
11. Astumian, R. D. The Unreasonable Effectiveness of Equilibrium Theory for Interpreting Nonequilibrium Experiments. *Am. J. Phys.* **2006**, *74*, 683–688.
12. Einstein, A.; Ehrenfest, P. Zur Quantentheorie des Strahlungsgleichgewichts. *Z. Phys.* **1923**, *19*, 301–306.
13. Coskun, A.; Banaszak, M.; Astumian, R. D.; Stoddart, J. F.; Grzybowski, B. A. Great Expectations: Can Artificial Molecular Machines Deliver on Their Promise? *Chem. Soc. Rev.* **2011**, *41*, 19–30.
14. Huxley, A. F. Muscle Structure and Theories of Contraction. *Prog. Biophys. Biophys. Chem.* **1957**, *7*, 255–318.
15. Ragazzon, G.; Baroncini, M.; Silvi, S.; Venturi, M.; Credi, A. Light-Powered Autonomous and Directional Molecular Motion of a Dissipative Self-Assembling System. *Nat. Nanotechnol.* **2014**, 10.1038/nnano.2014.260.
16. Astumian, R. D. Stochastic Conformational Pumping: A Mechanism for Free-Energy Transduction by Molecules. *Annu. Rev. Biophys.* **2011**, *40*, 289–313.
17. Astumian, R. D.; Derenyi, I. Fluctuation Driven Transport and Models of Molecular Motors and Pumps. *Eur. Biophys. J.* **1998**, *27*, 474–489.
18. Mukherjee, S.; Warshel, A. Electrostatic Origin of the Mechanochemical Rotary Mechanism and the Catalytic Dwell of F_1-ATPase. *Proc. Natl. Acad. Sci. U.S.A.* **2011**, *108*, 20550–20555.
19. Astumian, R. D.; Bier, M. Mechanochemical Coupling of the Motion of Molecular Motors to ATP Hydrolysis. *Biophys. J.* **1996**, *70*, 637–653.
20. Astumian, R. D. Irrelevance of the Power-Stroke for the Directionality, Stopping Force, and Optimal Efficiency of Chemically Driven Molecular Machines. *Biophys. J.* **2015** in press.
21. Carter, N. J.; Cross, R. A. Mechanics of the Kinesin Step. *Nature* **2005**, *435*, 308–312.

22. Berry, R. M. ATP Synthesis: The World's Smallest Wind-Up Toy. *Curr. Biol.* **2005**, *15*, R385–R387.
23. Vale, R. D.; Milligan, R. A. The Way Things Move: Looking under the Hood of Molecular Motor Proteins. *Science* **2000**, *288*, 88–95.
24. Liphardt, J. Single Molecules: Thermodynamic Limits. *Nat. Phys.* **2012**, *8*, 638–639.
25. Bustamante, C.; Cheng, W.; Mejia, Y. X. Revisiting the Central Dogma One Molecule at a Time. *Cell* **2011**, *144*, 480–497.
26. Chatterjee, M. N.; Kay, E. R.; Leigh, D. A. Beyond Switches: Ratcheting a Particle Energetically Uphill with a Compartmentalized Molecular Machine. *J. Am. Chem. Soc.* **2006**, *128*, 4058–4073.
27. Astumian, R. D. Thermodynamics and Kinetics of Molecular Motors. *Biophys. J.* **2010**, *98*, 2401–2409.